Nanomechanical properties of sputter-deposited HfO_2 and $Hf_xSi_{1-x}O_2$ thin films

D. K. Venkatachalam,[a] J. E. Bradby, M. N. Saleh, S. Ruffell, and R. G. Elliman
Department of Electronic Materials Engineering, Research School of Physics and Engineering, The Australian National University, Canberra ACT 0200, Australia

(Received 27 February 2011; accepted 23 July 2011; published online 29 August 2011)

The mechanical properties of sputter-deposited HfO_2 and $Hf_xSi_{1-x}O_2$ films were studied as a function of composition using nanoindentation. The elastic modulus and hardness were measured at room temperature for as-deposited films of varying Hf content and for films subjected to annealing at 1000 °C. The elastic modulus and hardness of as-deposited films were found to increase monotonically with increasing HfO_2 content, with the hardness increasing from 5.0 ± 0.3 GPa for pure SiO_2 to 8.4 ± 0.4 GPa for pure HfO_2. All films were found to be harder after annealing at 1000 °C, with the increase for SiO_2 films attributed to densification of the SiO_2 network and that for the $Hf_xSi_{1-x}O_2$ films to a combination of phase separation, densification, and crystallization. © *2011 American Institute of Physics*. [doi:10.1063/1.3627155]

I. INTRODUCTION

Hafnium-oxide (HfO_2)-based materials have drawn wide research interest due to their excellent optical and electrical properties. Pure hafnium oxide is a high refractive index, low absorption material used for dielectric mirrors and optical coatings and, in combination with silicon dioxide in the form of hafnium silicate ($Hf_xSi_{1-x}O_2$), is used to produce optical coatings with high laser damage thresholds.[1,2] Hafnium oxide is also of interest as a replacement for silicon dioxide in microelectronic applications due to its high dielectric-constant ($k \sim 25$) and its interface stability with silicon. The use of high-k dielectrics is critical for future microelectronic-scaling to reduce gate leakage and dielectric breakdown and increase the capacitance density and voltage linearity in metal-insulator-metal (MIM) capacitors. However, the low crystallization temperature of pure amorphous hafnium oxide films is a limitation in this application, as current CMOS processing requires film stability during annealing to 1000 °C for 5 s.[3–6] Emerging devices therefore employ amorphous hafnium silicate films, which have a higher crystallization temperature.[7,8]

The electrical and optical properties of HfO_2 and $Hf_xSi_{1-x}O_2$ thin films have been widely investigated, and considerable effort has been devoted to understand the preparation and thermal stability of such films.[5,8–10] In contrast, very little has been reported on the mechanical properties of these materials, even though such properties are of critical importance for many applications. For example, the elastomechanical response and process-induced stress evolution of the high-k dielectric films during thermal cycling has a direct effect on process integration and long-term reliability. The dielectric in high-k MIM capacitors is stressed by Coulomb interactions between the charges on the two electrodes, causing capacitance-voltage nonlinearity, an effect called Maxwell stress (σ_{ms}),[11] which depends on the elastic properties of the dielectric thin film. Thus, knowledge of the mechanical properties of the dielectric film is clearly important in understanding and modeling such behavior.

In this study, we have used nanoindentation to measure the hardness and elastic modulus of sputter-deposited HfO_2 and $Hf_xSi_{1-x}O_2$ thin films. Nanoindentation is an established tool for the measurement of hardness and elastic modulus of surfaces and thin films.[12] Its attractiveness stems from the fact that mechanical properties at small scales can be determined directly from the indentation load and displacement measurements without the need to image the residual impression. Such measurements are commonly performed with a Berkovich three-sided pyramid indenter tip (face angle of 65.3°), but here the measurements are performed with a sharper cube-corner tip (face angle of 35.3°). Cube-corner tips induce plastic deformation in thin films at lower indentation loads than Berkovich tips. The films used in this study are of a thickness range 100–150 nm deposited on a silicon substrate. This system is similar to investigating a soft-film on a harder substrate, in which high indentation loads will have a significant contribution from the underlying substrate. Also, Chudoba *et al.*[13] have shown that reliable thin-film hardness and modulus values can be measured with cube-corner tips by an appropriate choice of unload data fit range.

II. EXPERIMENTAL DETAILS

HfO_2 and $Hf_xSi_{1-x}O_2$ films were deposited onto 100 mm diameter, prime-grade p-type Si (100) wafers at room temperature by radio frequency (RF) sputtering using a commercial sputter deposition system (AJA International ATC 2400-V). The deposition chamber was evacuated to a pressure of 0.133 mPa and back-filled with Ar gas to a pressure of 0.53 Pa for deposition. Pure (99.99%) HfO_2 and SiO_2 targets were used as source materials, and the composition of the films was varied from pure HfO_2 to pure SiO_2 by varying the relative deposition rates of the HfO_2 and SiO_2 sources. The average deposition rate was maintained at around 1.3 nm/s, and

[a]Author to whom correspondence should be addressed. Electronic mail: Dinesh.Venkatachalam@anu.edu.au.

the wafer was rotated at 25 rpm during deposition to achieve uniform thickness across its 100 mm diameter. After deposition, the wafers were diced into 1×1 cm square samples, with one sample of each film composition subsequently subjected to thermal annealing at 1000 °C for 60 min in a quartz-tube furnace. The furnace tube was flushed with Ar at a flow rate of 1650 ml/min and sealed from the atmosphere by passing the Ar gas through an oil-filled backflow preventer at the tube exit. The Ar was dried prior to entering the furnace by passing it through a laboratory drying canister filled with anhydrous $CaSO_4$.

The composition and thickness of as-deposited and annealed films were measured by Rutherford backscattering spectrometry (RBS) using 2 MeV He^+ ions incident normal to the sample surface and detected with a surface-barrier detector at a scattering angle of 168°. The thickness and refractive index of the films was also measured using a spectroscopic ellipsometer. The crystal structure of the films was determined by glancing-incidence x ray diffraction (GI-XRD) using a Panalytical Xpert Pro™ system with Cu Kα radiation at 1.545 Å. The angle of incidence of the monochromated x ray beam was maintained at 0.5° to the sample surface to minimize contributions from the Si substrate.

The mechanical properties of the films were determined from nanoindentation measurements using a Hysitron Triboindenter™ fitted with a cube-corner diamond tip. Fifty indents were performed on each sample within a load range between 10 and 1200 μN to obtain data at a range of maximum depths. The elastic modulus and hardness were determined by analyzing individual load-unload curves using the Oliver-Pharr method.[14] The technique uses the slope of the tangent to the unloading data at maximum load in conjunction with the derivative of the elastic equations of contact for an equivalent conical indenter to determine the depth of the circle of contact (contact depth). Once this is known, the contact area is extracted from the tip area function, allowing the mechanical parameters to be extracted. Many indent curves are measured over a range of maximum loads to extract depth profiles of modulus and hardness. The tip area function and compliance was generated by indentation in fused silica immediately after the nanoindentation data on the samples was collected. The calibration parameters were confirmed by measuring the mechanical properties of both fused silica and crystalline silicon using the identical experimental set-up. The mechanical properties are well known, allowing the area to be extracted as a function of contact depth. The Oliver-Pharr method is well established but requires slight modification when not using the conventional Berkovich type indenters. The tangent to the unloading data is determined by first fitting the unloading data with a power law curve, thus allowing the tangent to be calculated. The recommended range of the unloading data to use for fitting is 80% (0.9 to 0.1 of maximum load). However, Chudoba *et al.*[13] found that features sometimes observed in the unloading data from indents made using a cube corner caused inaccurate fitting. Therefore, to ensure reliable hardness and modulus data when using a cube corner tip, fitting should be performed using only the upper portion of the unloading curve. In this study, the upper 95%-60% of data from the unloading curve was used to calculate the hardness and modulus.

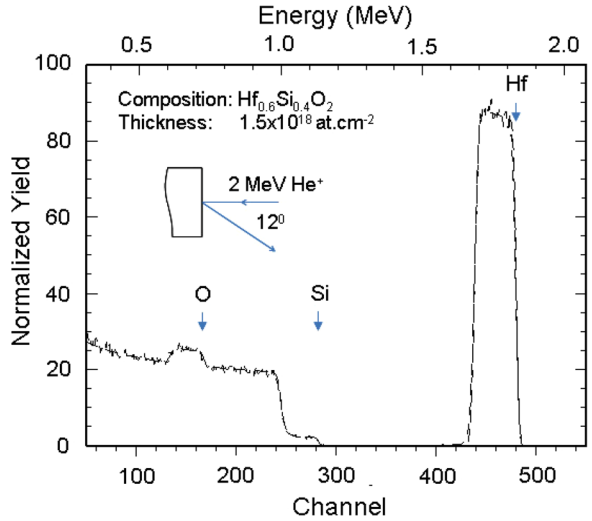

FIG. 1. (Color online) RBS spectrum of an as-deposited $Hf_xSi_{1-x}O_2$ film on a Si substrate together with a theoretical fit to the data from the RUMP code. The composition and thickness of this particular film were determined to be $Hf_{0.6}Si_{0.4}O_2$ and 1.5×10^{18} at.cm^{-2} and 194 nm, respectively.

III. RESULTS AND DISCUSSION

Figure 1 shows a typical RBS spectrum for an as-deposited $Hf_xSi_{1-x}O_2$ film together with a fit to the experimental data using the RUMP code.[15] The fit is consistent with a film of composition $Hf_{0.6}Si_{0.4}O_2$ and thickness 194 nm. (NB: The thickness of the film was determined by assuming a mixture of HfO_2 and SiO_2 with bulk densities, 9.68 g.cm^{-3} and 2.26 g.cm^{-3}, respectively. In this example, the film thickness was determined to be 1.5×10^{18} atoms.cm^2, which corresponds to 194 nm when bulk densities are assumed.) RBS analysis of samples after annealing at 1000 °C showed that there was no significant change in the composition of the films.

Table I summarizes the composition and thickness of as-deposited films. The four compositions are labeled as A-D, respectively. The nominal compositions and thicknesses of the films are based on *in situ* measurements of the HfO_2 and SiO_2 deposition rates using an *in situ* crystal-oscillator. Actual compositions were determined from RBS data, such as that shown in Fig. 1, while film thicknesses were determined from RBS and ellipsometry measurements. The thicknesses measured by the two techniques are in excellent agreement, with differences being within the

TABLE I. Summary of the film composition and thickness measured by Rutherford backscattering spectrometry and spectroscopic ellipsometry.

			Measured thickness (nm)	
Thin film	Nominal x	Measured by RBS[a] x	Ellipsometer	RBS[a]
HfO_2 (A)	1.00	1.00 ± 0.05	159 ± 4	154 ± 8
$Hf_xSi_{1-x}O_2$ (B)	0.75	0.83 ± 0.04	138 ± 3	140 ± 7
$Hf_xSi_{1-x}O_2$ (C)	0.50	0.60 ± 0.03	208 ± 5	194 ± 10
SiO_2 (D)	0.00	0.00	118 ± 3	110 ± 6

[a]Assumed bulk density of $HfO_2 = 9.68$ g.cm^{-3} and $SiO_2 = 2.26$ g.cm^{-3}.

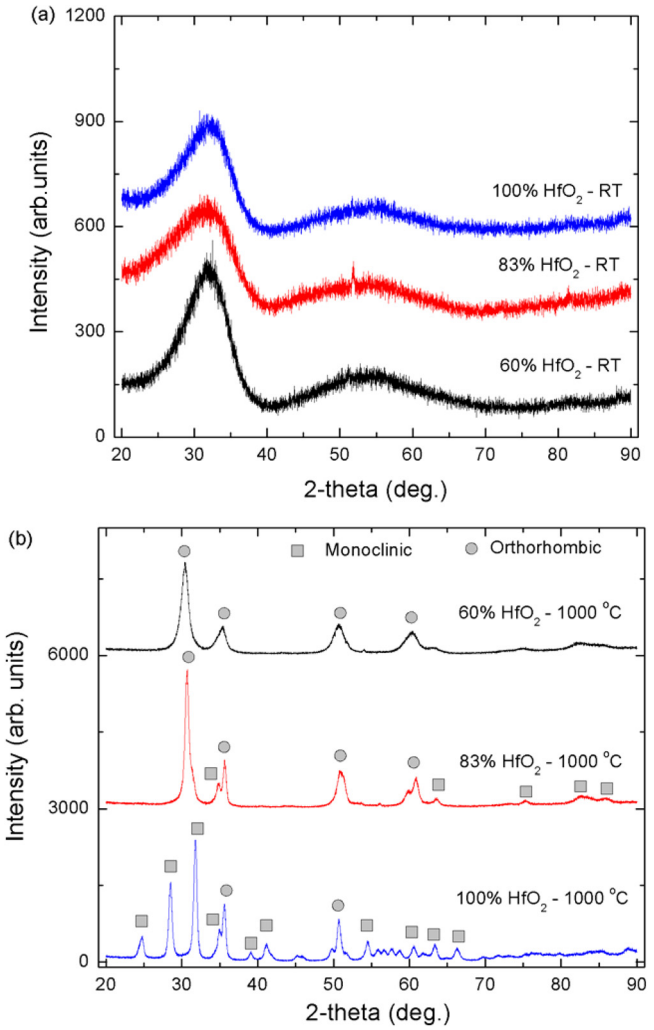

FIG. 2. (Color online) (a) GI-XRD spectra for as-deposited HfO_2 and $Hf_xSi_{1-x}O_2$ films and (b) GI-XRD spectra for films after annealing at 1000 °C. The location of diffraction peaks corresponding to the monoclinic and orthorhombic phases of HfO_2 are indicated by symbols.

uncertainty of the measurements. Note that the error associated with RBS measurements is estimated to be around 5% for both the thickness and composition, while that for the ellipsometry is estimated to be 2%.

GI-XRD spectra from as-deposited and annealed samples are shown in Fig. 2. The spectra from as-deposited films (presented in Fig. 2(a)) exhibit broad peaks centered at 2θ values of 32° and 55°, consistent with the films being amorphous. In contrast, spectra from the annealed samples (presented in Fig. 2(b)) show well-defined diffraction peaks from HfO_2. This is consistent with previous studies, in which $Hf_xSi_{1-x}O_2$ films have been shown to undergo phase separation during annealing to produce crystalline HfO_2 precipitates within an amorphous SiO_2 matrix. Indexing the diffraction patterns shows that the annealed HfO_2 film is composed primarily of the monoclinic phase (~90% vol. fraction), with a smaller volume fraction of the orthorhombic phase (10% vol. fraction), while the annealed $Hf_xSi_{1-x}O_2$ films are composed mainly of the orthorhombic phase (~70% vol. fraction) and a smaller volume fraction of the monoclinic phase (30% vol. fraction). From this data and results from previous studies,[16–18] it is clear that, while

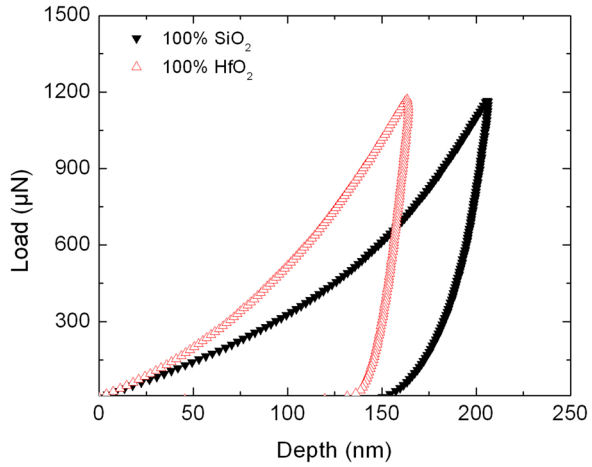

FIG. 3. (Color online) Typical nanoindentation load-unload curves for as-deposited SiO_2 and HfO_2. The measurements were made using a sharp corner cube tip with loading and unloading times of 0.5 s each.

as-deposited films can be regarded as a homogenous mixture of HfO_2 and SiO_2, annealed $Hf_xSi_{1-x}O_2$ are composites of c-HfO_2 in an amorphous SiO_2 matrix and annealed HfO_2 films have a mixed phase crystalline structure.

Typical nanoindentation load-unload curves are shown in Fig. 3. For a maximum indentation load of 1200 μN, the depth of penetration in HfO_2 and SiO_2 was found to be 155 nm and 205 nm, respectively, comparable to or greater than the film thickness. The smooth load-displacement curve suggests that no cracking or delamination of the films was induced by the indentation process.

Figure 4 shows the reduced elastic modulus (E) and hardness (H) measured as a function of indentation contact depth (h_c) for each of the films. Measurements at low loads, contact depths less than ~25 nm, show very high E and H values that are generally attributed to indentation size effects[13,19] and difficulties with obtaining accurate tip area functions. Hardness increase toward the surface due to indentation size effect depends on the preparation of the films, indenter tip radius, and agglomeration of dislocations at the very beginning of the plastic deformation. The measured hardness gradient in the low depth range is, therefore, inevitably a combination of several effects. At higher loads, contact depths greater than 50 nm, the modulus of the thinner SiO_2 film gradually increases with increasing depth. Such effects arise from increasing contributions from the substrate. Interestingly, the extracted hardness values seem less sensitive to the penetration depth, remaining reasonably constant for penetration depths over the range 50–150 nm. In order to summarize the mechanical properties, E and H values were determined by averaging measurements over the contact depth in the range 50 to 100 nm in this study. The validity of this approach is supported by the fact that the measured modulus of deposited SiO_2 is similar to that measured for bulk SiO_2, and comparison of data extracted over other ranges had little effect on the results.

The extracted elastic modulus values are shown in Fig. 5(a) as a function of the film composition. The modulus of the as-deposited films increases with increasing Hf content, from around 68 ± 4 GPa for SiO_2 to 152 ± 13 GPa for HfO_2.

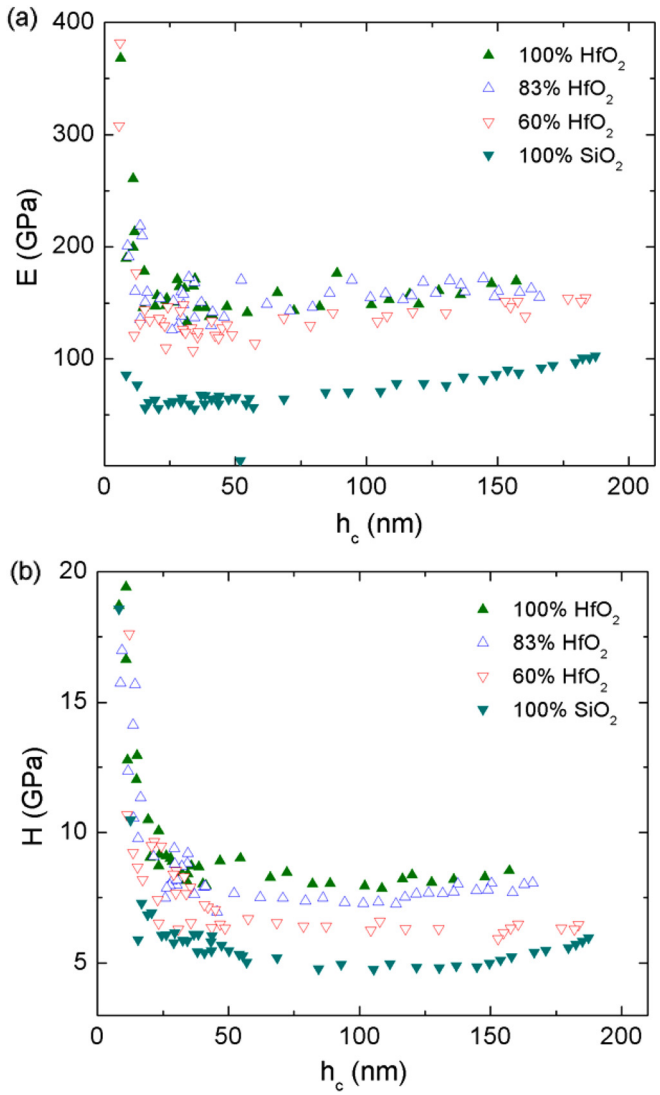

FIG. 4. (Color online) Plots of (a) modulus E and (b) hardness H vs indenter penetration h_c for as-deposited HfO_2 and $Hf_xSi_{1-x}O_2$ films on a Si substrate. Data have been corrected for thermal drift and instrument compliance, and data to create tip area function was generated immediately after the samples were probed.

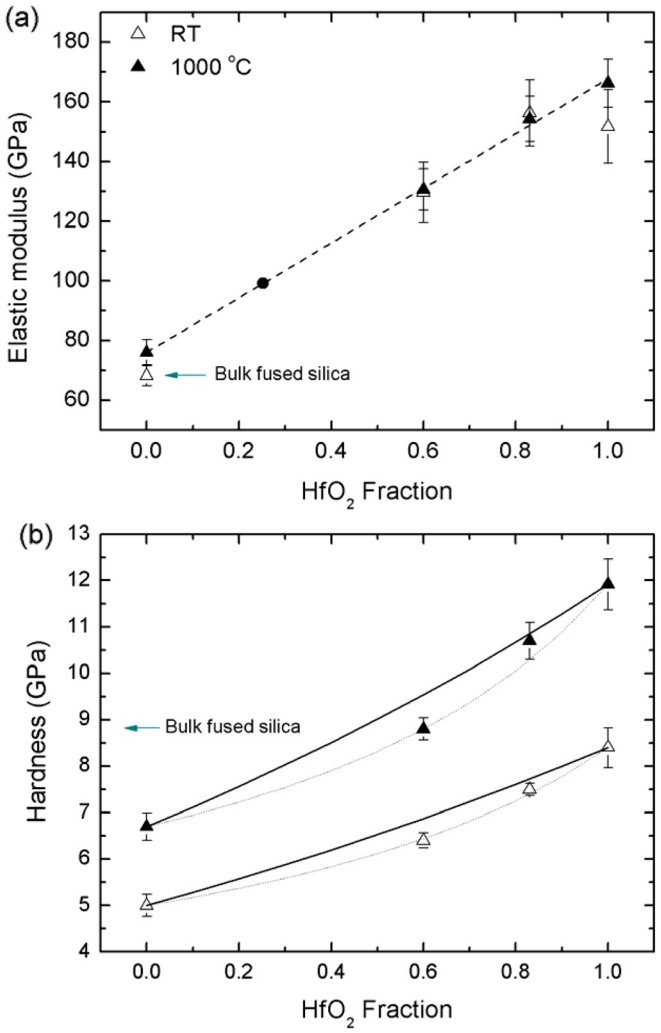

FIG. 5. (Color online) (a) Elastic modulus extracted from nanoindentation load-unload curves as a function of the molecular fraction of HfO_2. The dashed line is a linear fit to the data. (b) Calculated hardness as a function of the molecular fraction of HfO_2. Data is shown for as-deposited (open symbols) and annealed (closed symbols) films. The solid and dashed lines represent upper and lower bounds on the hardness calculated from iso-strain and iso-stress models, respectively.

In contrast to SiO_2, Hf oxides and silicates interact strongly with diffusing oxygen during deposition. This interaction occurs throughout the bulk of the film, thereby increasing the density of the films.[20] This increase in density contributes to the increase in hardness and modulus values of the as-deposited films. A similar trend is observed for the annealed films, with the modulus increasing from 76 ± 4 GPa for SiO_2 to 166 ± 8 GPa for HfO_2. Within the measurement error, no difference in the modulus was observed after annealing; however, the modulus was observed to increase linearly with increasing HfO_2 content.

Extracted hardness values are shown in Fig. 5(b) as a function of the film composition. The data show a monotonic increase in hardness with increasing HfO_2 content and an increase in the hardness of films with the same composition after annealing at 1000 °C. The solid and dashed lines represent upper and lower bounds on the hardness as calculated from iso-strain and iso-stress models of a two-component composite, i.e., an upper bound of $H_{max} = f_h H_h + f_s H_s$ and a lower bound of $H_{min} = H_h H_s/(f_h H_h + f_s H_s)$, where f_h and H_h are the volume fraction and hardness of pure HfO_2 and f_s and H_s are the volume fraction and hardness of pure SiO_2.

The hardness of the as-deposited SiO_2 film was measured to be 5.0 ± 0.3 GPa, considerably lower than that of the bulk-fused silica reference sample, which is expected, given that deposited films are generally less dense than bulk material. The hardness of this film increased to 6.7 ± 0.3 GPa after annealing at 1000 °C, consistent with some densification of the film. In contrast, the increase in the hardness of the HfO_2 film is most likely associated with crystallization of the film, which transforms from an amorphous phase to a mixture of monoclinic and orthorhombic phases. This also involves densification of the film, as the crystalline phases are generally more dense (density 9.68 g/cm^{-2}) than the amorphous phase (density 9.38 g/cm^3), with stable monoclinic phase being denser than the metastable orthorhombic phase.[21] On this basis, the increase in hardness of the $Hf_xSi_{1-x}O_2$ films after annealing is attributed to phase separation of the SiO_2 and HfO_2, densification of the SiO_2, and crystallization

of the HfO_2 fraction to form a composite material. The data in Fig. 5(b) for as-deposited and annealed samples are well described by the iso-stress model, which is to be expected given their microstructure.

IV. CONCLUSIONS

The elastic modulus and hardness of amorphous $Hf_xSi_{1-x}O_2$ thin films deposited by sputter deposition have been shown to increase monotonically with increasing Hf content, with the hardness increasing from 5.0 ± 0.3 GPa for $x = 0$ (pure SiO_2) to 8.4 ± 0.4 GPa for $x = 1$ (pure HfO_2). All films were shown to be harder after annealing at 1000 °C, with the increase for SiO_2 films attributed to densification of the SiO_2 network and that for the $Hf_xSi_{1-x}O_2$ films to a combination of phase separation, densification, and crystallization.

ACKNOWLEDGMENTS

The authors wish to acknowledge the Australian Research Council (ARC) for financial support. J.E.B. wishes to further acknowledge the ARC for QEII Fellowship.

[1]W. T. Liu, Z. T. Liu, F. Yan, and T. T. Tan, Physica B **405**(4), 1108 (2010).
[2]C. J. Stolz, L. M. Sheehan, M. K. von Gunten, R. P. Bevis, and D. J. Smith, in *Advances in Optical Interference Coatings*, edited by C. Amra and A. Macleod (SPIE, Bellingham, WA, 1999), Vol. 3738, p. 318.
[3]Y. C. Quan, J. E. Lee, H. Kang, Y. Roh, D. Jung, and C. W. Yang, Jpn. J. Appl. Phys. **41**(11B), 6904 (2002).
[4]F. Fillot, B. Chenevier, S. Maîtrejean, M. Audier, P. Chaudouët, B. Bochu, J. P. Sénateur, A. Pisch, T. Mourier, H. Monchoix, B. Guillaumot, and G. Passemard, Microelectron. Eng. **70**(2–4), 384 (2003).
[5]R. Nahar, V. Singh, and A. Sharma, J. Mater. Sci.: Mater. Electron. **18**(6), 615 (2007).
[6]S. Lee, W. G. Kim, S. W. Rhee, and K. Yong, J. Electrochem. Soc. **155**(2), H92 (2008).
[7]J. Morais, L. Miotti, G. V. Soares, S. R. Teixeira, R. Pezzi, K. P. Bastos, I. J. R. Baumvol, A. L. P. Rotondaro, J. J. Chambers, M. R. Visokay, and L. Colombo, Appl. Phys. Lett. **81**(16), 2995 (2002).
[8]P. R. Chalker, P. A. Marshall, R. J. Potter, T. B. Joyce, A. C. Jones, S. Taylor, T. C. Q. Noakes, and P. Bailey, J. Mater. Sci.: Mater. Electron. **15**(11), 711 (2005).
[9]I. Z. Mitrovic, O. Buiu, S. Hall, C. Bungey, T. Wagner, W. Davey, and Y. Lu, Microelectron. Reliab. **47**(4–5), 645 (2007).
[10]S. W. Nam, J. H. Yoo, S. Nam, H. J. Choi, D. Lee, D. H. Ko, J. H. Moon, J. H. Ku, and S. Choi, J. Non-Cryst. Solids **303**(1), 139 (2002).
[11]C. Wenger, G. Lupina, M. Lukosius, O. Seifarth, H. J. Muessig, S. Pasko, and C. Lohe, J. Appl. Phys. **103**(10), 104103 (2008).
[12]S. Bec, A. Tonck, and J. L. Loubet, Philos. Mag. **86**(33), 5347 (2006).
[13]T. Chudoba, P. Schwaller, R. Rabe, J. M. Breguet, and J. Michler, Philos. Mag. **86**(33), 5265 (2006).
[14]W. C. Oliver and G. M. Pharr, J. Mater. Res. **7**(6), 1564 (1992).
[15]See http://www.genplot.com for information about comprehensive analysis and simulation of RBS spectra.
[16]J. H. Ha, D. Chi, and P. C. McIntyre, Appl. Phys. Lett. **85**(24), 5884 (2004).
[17]R. Ludeke and E. Gusev, J. Appl. Phys. **96**(4), 2365 (2004).
[18]P. Broqvist and A. Pasquarello, Microelectron. Eng. **84**(9–10), 2416 (2007).
[19]W. W. Gerberich, N. I. Tymiak, J. C. Grunlan, M. F. Horstemeyer, and M. I. Baskes, J. Appl. Mech. **69**(4), 433 (2002).
[20]L. V. Goncharova, M. Dalponte, T. Feng, T. Gustafsson, E. Garfunkel, P. S. Lysaght, and G. Bersuker, Phys. Rev. B **83**(11), 115329 (2011).
[21]C. T. Kuo, R. Kwor, and K. M. Jones, Thin Solid Films **213**(2), 257 (1992).